Phonon Lifetimes and Thermal Conductivity of the Molecular Crystal α-RDX

Gaurav Kumar, Francis G. VanGessel, Daniel C. Elton & Peter W. Chung

Department of Mechanical Engineering, University of Maryland, College Park, Maryland USA

ABSTRACT

The heat transfer properties of the organic molecular crystal α-RDX were studied using three phonon scattering based thermal conductivity models. It was found that the widely used Peierls-Boltzmann model for thermal transport in crystalline materials breaks down for α-RDX. We show this breakdown is due to a large degree of anharmonicity that leads to a dominance of diffusive-like carriers. Despite being developed for disordered systems, the Allen-Feldman theory for thermal conductivity actually gives the best description of thermal transport. This is likely because diffusive carriers contribute to over 95% of the thermal conductivity in α-RDX. The dominance of diffusive carriers is larger than previously observed in other fully ordered crystalline systems. These results indicate that van der Waals bonded organic crystalline solids conduct heat in a manner more akin to amorphous materials than simple atomic crystals.

INTRODUCTION

RDX ($C_3H_6N_6O_6$) is an organic compound which has high energy density and low sensitivity to external stimuli, making it suitable for use in various military and industrial applications as a secondary explosive (SE). Under atmospheric conditions, RDX is in the α crystal phase whose unitcell has 168 atoms which in turn has 504 phonon branches [1]. Forming a more complete understanding of phonon dynamics in complex molecular crystals, such as the energetic α-RDX, is of fundamental importance due to the role that phonons play in initiation mechanisms of energetics [2, 3]. In molecular crystals, commonly used in energetics, phonons facilitate the formation of the microscale reaction zones, i.e. hotspots, wherein the flow of energy into key vibrational modes initiates the chemical decomposition process [2, 4, 5]. However, open questions remain as to the exact mechanism through which intermodal and spatial energy transfer occurs in molecular crystals. Dlott et al. postulated a multiphonon up-pumping

mechanism to explain the intermodal energy transfer phenomenon, while other works speculated that the energy transfer process occurs through a direct route [2, 3]. Furthermore, there exists a relative lack of knowledge regarding how thermal energy is conducted in van der Waals bonded organic molecular crystals in relation to "simple" atomic crystalline materials such as Si or Ge. Highlighting the possible shortcomings of the existing kinetic theory for thermal transport in molecular crystals is the extremely low thermal conductivity of α-RDX, TATB, and β-HMX, ≤ 1 W/m·K [6, 7]. Such values are more akin to conductivities observed in amorphous or glassy materials than in atomic crystalline systems. A similar phenomenon of ultralow thermal conductivity has been observed in certain inorganic perovskite and selenide compound crystals [8, 9]. Theoretical and experimental studies of both of these systems have shown a breakdown of Peierls-Boltzmann theory [9, 10, 11], which is based on a partial Hamiltonian and breaks down when the full crystal Hamiltonian is sufficiently anharmonic [12]. Peierls-Boltzmann is a popular approach for calculation of bulk thermal conductivity in crystalline solids, often calculated through the so-called phonon gas model (PGM). The breakdown of the PGM in the perovskite and selenide compounds has been linked to the strong anharmonicity present in those systems. Molecular crystals, notably RDX, possess similarly large unit cells that generally have a highly anharmonic Hamiltonian. Therefore, the PGM, as well as alternative thermal conductivity models, must be evaluated for their accuracy in modelling phonon mechanisms in molecular crystals. Only then will it be possible to elucidate the manner in which phonons store, transport, and transfer energy in complex molecular crystalline systems.

In this paper we evaluate the strength of anharmonic coupling in the molecular crystal α-RDX via the phonon linewidths and lifetimes. Subsequently, using harmonic and anharmonic phonon properties, we evaluate three thermal conductivity models, namely the PGM, Cahill Watson and Pohl (CWP) model, and Allen and Feldman (AF) model. We assess the accuracy of these models in estimating the thermal conductivity of α-RDX by comparing with values obtained from Green-Kubo molecular dynamics (GK-MD) [6]. The PGM has been shown to give excellent predictions of bulk thermal conductivity in a wide range of simple atomic crystalline systems [13, 14]. In contrast, the CWP model was initially developed for application to weakly disordered (i.e. mixed species) crystals [15], but has shown to give better predictions than the PGM model for certain Se compounds [9]. Finally, the theory of Allen and Feldman [16] was initially developed for disordered phases in which heat transfer is diffusive in nature. However, it has been shown that significant heat currents may be carried by diffusive modes in certain "complex" crystalline materials [10].

In the next section, we present the methodology for calculating phonon linewidths, lifetimes, frequencies, and group velocities. We then apply this methodology, analysing the phonon lifetimes of α-RDX and calculating the thermal conductivity predictions of the PGM, CWP, and AF models respectively. In the final section we present our conclusions on the presented results and discuss what they reveal about thermal transport in this unique material.

METHODOLOGY

Phonon relaxation times

Accurate prediction of properties like thermal conductivity require knowledge of anharmonic vibrational properties of the material, in particular phonon lifetimes. Furthermore, the degree of anharmonicity present in a crystalline system may be used to determine the validity of the PGM [9, 10]. In this study we use the normal mode

decomposition (NMD) method to determine the phonon lifetimes for all branches. The NMD approach is computationally more efficient than other techniques [17] and has been used successfully for many ordered materials such as silicon [18] and carbon nanotubes [19]. Here we give a brief overview of the methodology, while further details can be found in our earlier work [20]. Following the procedure laid out by Larkin [17] we calculate the mode projected phonon spectral energy density (SED) as

$$\Phi(\boldsymbol{k}, \omega) = \left| \frac{1}{\sqrt{2\pi}} \int_{-\infty}^{\infty} \dot{q}_\phi \, exp(-i\omega t) \, dt \right|^2 . \qquad 1)$$

Here $\dot{q}_\phi(t)$ is the time derivative of the phonon normal mode coordinate, ϕ is the phonon mode index and ω is the phonon mode frequency. In order to calculate $\dot{q}_\phi(t)$, a molecular dynamics simulation of a supercell size $N = 2 \times 2 \times 2 = 8$ was performed using open source package LAMMPS [21]. A 1 fs timestep was chosen (less than $\frac{1}{10}th$ of the smallest time period of atomic vibration in α-RDX) and the system was equilibrated for 2 ns under NPT conditions followed by data collection for another 2 ns under NVE conditions. The SED for each mode can be expressed as [17]

$$\Phi_\phi(\boldsymbol{k}, \omega) = C_{o\phi1} \frac{\frac{\Gamma_\phi}{\pi}}{(\omega_\phi - \omega)2 + \Gamma_\phi^2} + C_{o\phi2} \frac{\frac{\Gamma_\phi}{\pi}}{(\omega_\phi + \omega)2 + \Gamma_\phi^2} . \qquad (2)$$

where $\quad C_{o\phi1} = \sum_j \sum_{j'} cos[\omega(t_j - t_{j'})] \, A_{j\phi} \, A_{j'\phi} \frac{\omega_{o\phi} + \Gamma_\phi^2}{8 \, \tau_\phi \Gamma_\phi}$

and $\quad C_{o\phi2} = \sum_j \sum_{j'} cos[\omega(t_j - t_{j'})] \, B_{j\phi} \, B_{j'\phi} \frac{\omega_{o\phi} + \Gamma_\phi^2}{8 \, \tau_\phi \Gamma_\phi}$

where the phonons in each mode are indexed by j, Γ_ϕ is phonon linewidth, and $A_{j\phi}$, $A_{j'\phi}$, $B_{j\phi}$ and $B_{j'\phi}$ are the associated constants denoting growth and decay of phonon population [17]?. When $\omega \approx \omega_\phi$, $C_{o\phi1}$ becomes large and the term involving $C_{o\phi2}$ can be neglected. Under this approximation, SED for each mode contains a single peak which was fit to a Lorentzian function [20].The phonon relaxation time can then be extracted from the SED linewidth, Γ_ϕ, using the relation $\tau_\phi = 1/(2\Gamma_\phi)$.

Harmonic phonon properties

In addition to the anharmonic properties discussed above, several harmonic phonon properties are required in order to calculate thermal conductivity. These are the phonon frequencies, ω_ϕ, group velocities, $\boldsymbol{v}_\phi$, and specific heat, C_ϕ. The phonon frequencies are obtained using the harmonic lattice dynamics approach implemented in the open source package GULP [22]. The group velocities are calculated from the frequencies using a central difference scheme. The specific heat is determined from the relation

$$C_\phi = \frac{\hbar^2 \omega_\phi^2}{k_B T^2} \frac{\exp\left(\frac{\hbar\omega_\phi}{k_B T}\right)}{\left[\exp\left(\frac{\hbar\omega_\phi}{k_B T}\right) - 1\right]^2} \qquad 3)$$

where $\hbar$ is reduced Planck's constant, k_B is Boltzmann constant, and T is temperature. From the group velocity and the phonon lifetime, the phonon mean free path (MFP) can be calculated using $\Lambda_\phi = v_\phi \tau_\phi$, where $v_\phi = |\boldsymbol{v}_\phi|$. Further information regarding

calculation of these properties may be found in [23]. We used Smith and Bharadwaj flexible molecule potential [24] to calculate all phonon properties because of its ability to capture intramolecular vibrations and low computational cost as compared to reactive models or electronic structure methods. This potential has been successfully used to calculate thermal conductivity of α-RDX 0.378 W/m-K [6] which agrees qualitatively with experimental measurement of 0.193 W/m-K [25].

RESULTS & DISCUSSION

Phonon anharmonicity in α-RDX

Over 90% of the modes we studied were found to exhibit an SED curve with a clear single peak. This set includes modes where smaller peaks with heights less than 10% of the main peak value can at times be observed. The small peaks result from non-negligible $C_{o\phi2}$ term at frequencies considerably higher or lower than ω_ϕ. We believe the noise in SED data are MD simulation artefacts which can be a combination of under-thermalization, under-equilibration, and possible uncontrollable sources of noise. Phonon linewidths of the three acoustic phonon modes at the Γ point are zero and therefore phonon lifetimes for these three modes cannot be calculated using NMD technique. The following metrics were used to quantify the error in the Lorentzian fitting of all modes (except the 3 acoustic modes at Γ),

$$error_\phi = \sqrt{\frac{\sum_{l=1}^{n_d}(SED_{\phi l}-SED_{fit,\phi l})^2}{n_d}} \text{ , and } \% \, error = 100 \sqrt{\frac{\sum_{\phi=1}^{3n} error_\phi^2}{3n}} \bigg/ \sqrt{\frac{\sum_{\phi=1}^{3n}\sum_1^{n_d}(SED_\phi)^2}{3n \times n_d}}$$

where n_d is the number of data points in the SED of each mode, and $3n$ is the number of sampled phonon modes. Using this metric, we found $\% \, error = 2.61\%$ for RDX 2x2x2. Further, the standard deviation of $error_\phi$ is

$$\sigma_{fit} = 100 \sqrt{\frac{\sum_\phi^{3n}\left(error_\phi - \frac{\sum_\phi^{3n} error_\phi}{3n}\right)^2}{3n}} \bigg/ \frac{\sum_\phi^{3n} error_\phi}{3n} \text{ which was found to be } 0.66\%$$

indicating consistent good fit of SED across the modes. In Figure 1, the calculated phonon lifetimes are shown for each vibrational mode of α-RDX against frequency. Our results reveal that lifetimes in α-RDX decrease with increasing frequency up to ~3 THz, followed by flattening and subsequent overall increasing trend. In fact, some optical modes have lifetimes comparable to or even greater than lifetimes of acoustic modes. In
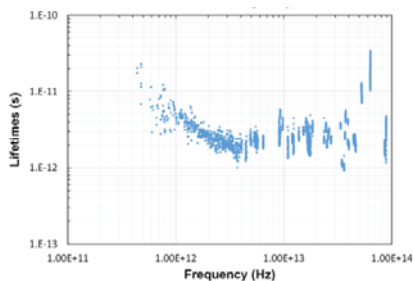

Figure 1 Phonon mode lifetimes of 2x2x2 supercell of α-RDX

2194

contrast, the acoustic modes of simple crystals such as silicon [18], carbon nanotubes [26] have the largest lifetimes while the optical modes have significantly smaller lifetimes. In fact, Callaway's model [27] for phonon lifetimes is an inverse relationship with ω.

The larger lifetimes of some optical modes are likely due to the large band gaps that exist in the band structure. Due to these large gaps, high frequency optical modes (>20 THz) participate in relatively fewer intrinsic phonon scattering events than lower frequency optical, and acoustic modes. A decrease in the number of allowed phonon-phonon interactions due to an increase in the acoustic-optical bandgap is similarly observed in III-V materials [28].

Note also that the magnitudes of the phonon lifetimes are quite low, on the order of 10 picoseconds, closer to lifetimes in amorphous solids than atomic crystals that have phonon lifetimes on the order of nanoseconds [18]. Lifetime values calculated in this study are in good agreement with vibron lifetimes in RDX which have been reported to fall in the range of 2.5 ps to 11 ps [29]. The short lifetimes indicate that RDX is a strongly anharmonic crystal.

Phonon gas model

The thermal conductivity based on PGM is obtained from a sum over the contributions of all phonon carriers, i.e.

$$\kappa_{PGM} = \sum_{\phi} C_{\phi} v_{\phi} \Lambda_{\phi}$$

4)

For an accurate calculation of the thermal conductivity we use a uniform sampling of $15 \times 15 \times 15$ wavevectors within the first Brillouin zone for calculation of the harmonic properties. Due to the relatively larger computational cost of calculating phonon lifetimes on a $15 \times 15 \times 15$ size RDX supercell, we took only the Γ point value. This simplification was justified in part through more refined calculations, where we saw that the average Γ point phonon lifetimes were within ~7% of the value at the BZ edge. Table I shows the predicted κ_{PGM} of α-RDX along 3 crystallographic directions a, b, and c using PGM, along with the GK-MD value [6]. As GK-MD does not curtail any phonon modes or sources of anharmonicity, we consider it a good source for the reference thermal conductivity to compare against alternative calculation approaches based on the same molecular potential. PGM clearly under-predicts the thermal conductivity of α-RDX by an order of magnitude. To understand the cause of this discrepancy we appeal to the underlying assumptions of the PGM, which assumes that a phonon wavepacket interacts only weakly with other phonons and therefore propagates a large distance before experiencing a scattering event. Quantitatively, this corresponds to the requirement that the phonon MFP be much larger than the lattice constant, i.e. the phonon wavepacket must "sample" the periodicity of the lattice [30]. In Figure 2 we plot the phonon MFP with respect to frequency and compare this value to the average lattice constant in RDX. Except for a relatively small fraction (< 1%) of low frequency phonon modes, the vast majority of carriers have a MFP smaller than the lattice constant, i.e. these carriers fall within the Ioffe-Regel regime [31]. Thus, for these *diffusive* carriers the PGM is *not* a valid descriptor for how they transport thermal energy and therefore under-predicts their contribution to thermal conductivity. We note that in [20] analysis of propagating and diffusive carrier contributions to thermal conductivity were calculated within the PGM framework. However, in that study the phonon lifetime was treated as a fitting parameter in order to match the GK-MD values of κ. It is clear that an accurate

thermal conductivity model for molecular crystals should account for the highly anharmonic, diffusive thermal carriers present in these systems. We now evaluate one

Table I. Thermal conductivity predictions of α-RDX from Green-Kubo MD and PGM, along the three principal crystallographic direction (values in units of W/m·K).

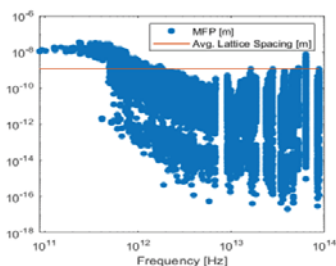|	a	b	c
κ_{PGM}	0.014	0.011	0.023
κ_{GK-MD}	0.387	0.353	0.394

Figure 2 Comparison of phonon MFP to average lattice spacing.

such model, namely the CWP model for minimum thermal conductivity.

Cahill-Watson-Pohl model

The CWP formula was initially developed to describe the low thermal conductivity observed in crystalline alloys where the lattice structure remains intact but there is randomness in regards to the species lying at each lattice site. It can account for the dispersive nature of the acoustic mode carriers. Recently, the CWP model has been successful in predicting a qualitatively accurate thermal conductivity versus temperature trend in a Se compound with zero disorder. The improvement over PGM was due to the treatment of carriers that fall below the Ioffe-Regel limit with the CWP model, while propagating carrier contributions were still calculated using the PGM. The CWP model for thermal conductivity is [15]

$$\kappa_{CWP} = \left(\frac{\pi}{6}\right)^{\frac{1}{3}} k_B n^{\frac{2}{3}} \sum_\lambda c_\lambda \left(\frac{T}{\theta_\lambda}\right)^2 \int_0^{\frac{\theta_\lambda}{T}} \frac{x^3 e^x}{(e^x - 1)^2} dx \ . \qquad 5)$$

where the sum is restricted to the 3 acoustic phonon branches, indexed by λ, c_λ is speed of sound, n is the number density of atoms, and $\theta_\lambda = v_\lambda \left(\frac{\hbar}{k_B}\right)(6\pi^2 n)^{\frac{1}{3}}$. Applying the CWP formula to αRDX yields a conductivity estimate of 0.167 W/m-K. This is still 50% of the averaged κ predicted using GK-MD which is ~0.378 W/m-K [6]. Although CWP performs markedly better than PGM, the disagreement with GK-MD is still relatively large. The cause is that the CWP model only accounts for the dispersion contributions in the three acoustic branches. However, due to the large number of optical modes, and small interband spacing, a significant fraction of heat is carried by the optical branches through coherence or non-diagonal effects [10, 12, 30]. This leads us to apply the AF model in order to account for such contributions to thermal transport in α-RDX.

Allen-Feldman model

Due to the majority of α-RDX carriers falling in the Ioffe-Regel regime, the phonons likely carry thermal energy in a manner more akin to amorphous solids than atomic crystals. To test this, we applied the theory of Allen and Feldman (AF) in which heat is assumed to move by coherences, i.e. interband effects. In this method κ is calculated from [16]

$$\kappa_{AF} = \frac{1}{V} \sum_{\phi} C_{\phi} D_{\phi} \qquad 6)$$

Here D_{ϕ} is mode diffusivity defined as

$$D_{\phi} = \frac{\pi V^2}{3\hbar^2 \omega_{\phi}^2} \sum_{\phi'}^{\phi' \neq \phi} |S_{\phi\phi'}|^2 \delta(\omega_{\phi} - \omega_{\phi'}) \qquad 7)$$

where $S_{\phi\phi'}$ is the off diagonal term of the heat current operator [12] and δ is the Dirac delta function that enforces energy conservation. The diffusivity is an intrinsic property of the normal modes and requires no assumption about the propagating nature of the phonons, such as in the PGM. We calculate the phonon mode diffusivity using a $3 \times 3 \times 3$ supercell in GULP [22]. Thermal conductivity from the AF approach is 0.354 W/m-K which is within 6% of the GK-MD estimate [6], see Table II below. The marked improvement of the AF prediction of κ relative to PGM and CWP indicates strongly that diffusive like carriers contribute to the majority of thermal transport in α-RDX.

Within the AF theory, we can break down the contributions to κ_{AF} by individual carrier's accumulation and by each carrier separately. These are shown respectively in Figure 3. We observe that the majority of heat is carried by low frequency phonon modes and the contribution from high frequency modes is negligible. According to Figure 3, 11% of the low frequency modes account for 90% of the total κ. We also found that ~70% of κ contribution can be attributed to optical mode phonons, primarily low frequency optical phonons which are neglected in the CWP model. This is a consequence of the fact that high frequency optical phonons have very small specific heat ($C_{\phi} \to 0$ when $\hbar\omega_{\phi} \gg k_B T$) which combined with their relatively small diffusivity results in very small contribution to κ. It is also interesting to note that the AF theory

Table II Comparison of κ predicted by various thermal conductivity models (unit W/mK)

κ_{GK-MD}	κ_{AF}	κ_{CWP}	κ_{PGM}	$\kappa_{AF} + \kappa_{PGM}$
0.378	0.354	0.167	0.017	0.371

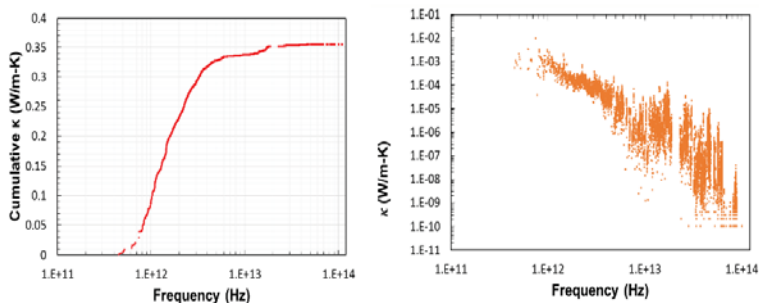
Figure 3. Cumulative and modal contributions to thermal conductivity with respect to frequency in α-RDX. Values calculated using Allen-Feldman theory.

considers heat transport purely due to the off-diagonal terms of heat current operator, which are non-propagating, while PGM considers heat transport via propagating phonon carriers (i.e. diagonal component). Within the unified approach [10], the propagating and non-propagating contributions are additive (termed the Peierls and coherence contributions respectively in that work). Thus, if we combine contributions from both κ_{AF} and κ_{PGM}, we obtain a thermal conductivity of 0.371 W/m·K which is within 2% the GK-MD prediction. Note that this comparison may suffer from insufficient BZ sampling as a $3 \times 3 \times 3$ supercell was used for AF approach while using $15 \times 15 \times 15$ grid of wavevectors was used for calculation of the propagating contribution. However, it is evident that both propagating and diffusive carriers contribute substantially to thermal transport in α-RDX, where the diffusive component is dominant, contributing 95% to the total thermal conductivity.

CONCLUSION

In this work we have presented our preliminary findings on the nature of thermal transport in the complex molecular crystal α-RDX. Analysis of the phonon linewidths and lifetimes indicate that α-RDX is a highly anharmonic crystal. The inability of the PGM to accurately estimate thermal conductivity indicates that the strong anharmonicity leads to a breakdown of the Peierls picture for thermal transport. Table II summarizes thermal conductivity calculated using the various approaches used in this study. For α-RDX, Allen-Feldman harmonic theory performs best. This result is intuitive as AF theory involves fewer assumption than PGM or CWP. We observed that low frequency optical phonons play a significant role in carrying heat in α-RDX. It is notable that these results suggest that diffusive carriers are the primary mechanism of heat transport in α-RDX, where propagating phonon modes contribute less than 5%. Similar phenomena involving a partitioning of thermal transport between diffusive and propagating modes has been previously observed in inorganic crystalline materials. However the relative contribution of diffusive carriers in α-RDX is significantly larger than previously observed in other crystalline systems. We suspect these observation regarding the nature of heat transfer in α-RDX will extend to other organic molecular crystals, particularly those with applications to energetics technology. In such systems, accurate description of thermal transport requires accounting for both acoustic and optical phonon bands, as well as both propagating and diffusive phonon modes.

ACKNOWLEDGMENTS

References

[1]   L. B. Munday, PhD Thesis, University of Maryland College Park, 2011.
[2]   D. D. Dlott and M. D. Fayer, *The Journal of Chemical Physics* 92 (6), 3798-3812 (1990).
[3]   B. Kraczek and P. W. Chung, *The Journal of Chemical Physics* 138 (7), 4505 (2013).
[4]   A. Tokmakoff, M. D. Fayer and D. D. Dlott, *Journal of Physical Chemistry* 97 (9), 1901-1913

(1993).

[5]   S. Ye, K. Tonokura and M. Koshi, *Chemical Physics* 293 (1), 1-8 (2003).

[6]   S. Izvekov, P. W. Chung and B. M. Rice, *International Journal of Heat and Mass Transfer* 54, 5623-5632 (2011).

[7]   M. P. Kroonblawd and T. D. Sewell, *Propellants, Explosives, Pyrotechnics* 41 (3), 502-513 (2016).

[8]   W. Lee, H. Li, A. B. Wong, D. Zhang, M. Lai, Y. Yu, Q. Kong, E. Lin, J. J. Urban and J. C. Grossman, *National Academy of Sciences* 114 (33), 8693-8697 (2017).

[9]   S. Mukhopadhyay, D. S. Parker, B. C. Sales, A. A. Puretzky, M. A. Mcguire and L. Lindsay, *Science* 360 (6396), 1455-1458 (2018).

[10] M. Simoncelli, N. Marzari and F. Mauri, *arXiv preprint arXiv:1901.01964,* 1-10 (2019).

[11] R. Peierls, in *Selected Scientific Papers Of Sir Rudolf Peierls: (With Commentary)*, edited by R. H. Dalitz and R. Peierls (Imperial College Press and World Scientific Publishing Co., Oxford, 1997), p. 15.

[12] R. J. Hardy, *Physical Review* 132 (1), 168-177 (1963).

[13] L. Lindsay, D. A. Broido and N. Mingo, *Physical Review B* 82 (11), 5427 (2010).

[14] L. Lindsay, D. A. Broido and T. L. Reinecke, *Physical Review B* 87 (16), 5201 (2013).

[15] D. G. Cahill, S. K. Watson and R. O. Pohl, *Phys. Rev. B* 46 (10), 6131-6140 (1992).

[16] P. B. Allen and J. L. Feldman, *Phys. Rev. B* 48 (17), 12581-12588 (1993).

[17] J. M. Larkin, PhD Thesis, Carnegie Mellon University, 2013.

[18] J. M. Larkin, McGaughey and A. J. H, *Journal of Applied Physics* 114 (2), 3507 (2013).

[19] J. A. Thomas, J. E. Turney, R. M. Iutzi, C. H. Amon and A. J. H. McGaughey, *Phys. Rev. B* 81 (8), 1411-1414 (2010).

[20] F. G. VanGessel, G. Kumar, D. C. Elton and P. W. Chung, *arXiv preprint arXiv:1808.08295,* 1-11 (2018).

[21] S. Plimpton, *J Comp Phys* 117, 1-19 (1995).

[22] J. D. Gale and A. L. Rohl, *Molecular Simulation* 29 (5), 291-341 (2003).

[23] F. G. VanGessel and P. W. Chung, *Computer Methods in Applied Mechanics and Engineering* 317, 1012-1036 (2017).

[24] G. D. a. B. R. K. Smith, *The Journal of Physical Chemistry B* 103 (18), 3570-3575 (1999).

[25] M. S. Miller, Report No. ARL-TR-1319, 1997.

[26] L. Lindsay, D. A. Broido and N. Mingo, *Phys. Rev. B* 80 (12), 5407 (2009).

[27] J. Callaway, *Phys. Rev.* 113 (4), 1046 (1959).

[28] L. Lindsay and D. A. Broido, *Journal of Physics: Condensed Matter* 20 (16), 1-6 (2008).

[29] S. Ye and M. Koshi, *The Journal of Physical Chemistry B* 110(37), 18515-18520 (2006).

[30] A. Auerbach and P. B. Allen, *Physical Review B* 29 (6), 2884-2890 (1984).

[31] A. F. Ioffe and A. R. Regel, in Progress in Semiconductors, edited by A. F. Gibson (John Wiley & Sons Inc., New York, 1960), p. 237.